

pubs.acs.org/est Article

# Decreases in Epoxide-Driven Secondary Organic Aerosol Production under Highly Acidic Conditions: The Importance of Acid—Base Equilibria

Madeline E. Cooke, <sup>∇</sup> N. Cazimir Armstrong, <sup>∇</sup> Alison M. Fankhauser, Yuzhi Chen, Ziying Lei, Yue Zhang, Isabel R. Ledsky, Barbara J. Turpin, Zhenfa Zhang, Avram Gold, V. Faye McNeill, Jason D. Surratt,\* and Andrew P. Ault\*



Cite This: Environ. Sci. Technol. 2024, 58, 10675-10684



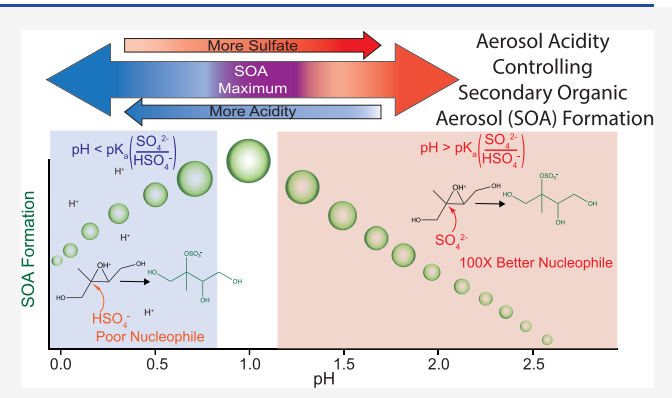
**ACCESS** 

III Metrics & More

Article Recommendations

Supporting Information

ABSTRACT: Isoprene has the highest atmospheric emissions of any nonmethane hydrocarbon, and isoprene epoxydiols (IEPOX) are well-established oxidation products and the primary contributors forming isoprene-derived secondary organic aerosol (SOA). Highly acidic particles (pH 0–3) widespread across the lower troposphere enable acid-driven multiphase chemistry of IEPOX, such as epoxide ring-opening reactions forming methyltetrol sulfates through nucleophilic attack of sulfate ( $\mathrm{SO_4}^{2-}$ ). Herein, we systematically demonstrate an unexpected decrease in SOA formation from IEPOX on highly acidic particles (pH < 1). While IEPOX-SOA formation is commonly assumed to increase at low pH when more [H<sup>+</sup>] is available to protonate epoxides, we observe maximum SOA formation at pH 1 and less SOA formation at pH



0.0 and 0.4. This is attributed to limited availability of  $SO_4^{2-}$  at pH values below the acid dissociation constant (p $K_a$ ) of  $SO_4^{2-}$  and bisulfate (HSO<sub>4</sub><sup>-</sup>). The nucleophilicity of HSO<sub>4</sub><sup>-</sup> is 100× lower than  $SO_4^{2-}$ , decreasing SOA formation and shifting particulate products from low-volatility organosulfates to higher-volatility polyols. Current model parameterizations predicting SOA yields for IEPOX-SOA do not properly account for the  $SO_4^{2-}/HSO_4^{-}$  equilibrium, leading to overpredictions of SOA formation at low pH. Accounting for this underexplored acidity-dependent behavior is critical for accurately predicting SOA concentrations and resolving SOA impacts on air quality.

KEYWORDS: atmospheric chemistry, aerosol acidity, multiphase chemistry, air pollution, climate change

## INTRODUCTION

Atmospheric aerosols impact both climate, through altering radiative forcing, <sup>1,2</sup> and public health, by increasing the risk for cardiovascular and respiratory diseases.<sup>3</sup> The impact of aerosols on climate and health is dependent on key chemical and physical properties, including particle acidity. <sup>1,4</sup> Aerosol particle acidity has been shown to impact reactivity through pH-dependent condensed-phase reactions, <sup>4–7</sup> as well as through effects on gas—particle partitioning, <sup>4,8–10</sup> with many reactions enhanced under highly acidic conditions. <sup>4,6,11,12</sup> Fine aerosol particles are expected to be acidic across the troposphere, with the most common pH range of pH 0–3. <sup>4,8,13</sup> Highly acidic aerosols (pH < 1) have been observed in areas across the globe, including the Eastern United States, <sup>14</sup> Hong Kong, <sup>15</sup> and Singapore, <sup>16</sup> and are predicted over a large fraction of the Earth's surface by global modeling. <sup>4</sup>

Secondary organic aerosol (SOA) is an abundant class of atmospheric fine particulate matter (PM<sub>2.5</sub>, particles with an aerodynamic diameter <2.5  $\mu$ m), accounting for over 50% of

organic aerosol mass globally. <sup>17</sup> A dominant SOA formation pathway results from the reaction of volatile organic compounds (VOCs) with atmospheric oxidants to produce lower volatility products that either nucleate or condense to the particle phase or undergo multiphase chemical reactions. <sup>17</sup> Isoprene ( $C_5H_8$ ) has the highest emissions of any nonmethane VOC to the atmosphere, <sup>18</sup> and is estimated to be one of the largest contributors to atmospheric SOA formation due to its high reactivity (i.e., containing two double bonds). <sup>19,20</sup> Through multiple oxidation steps with the atmospheric hydroxyl radical ( $\bullet$ OH) under low-nitric oxide (NO) conditions, isoprene forms lower volatility species that

Received: December 22, 2023 Revised: April 24, 2024 Accepted: May 28, 2024 Published: June 6, 2024





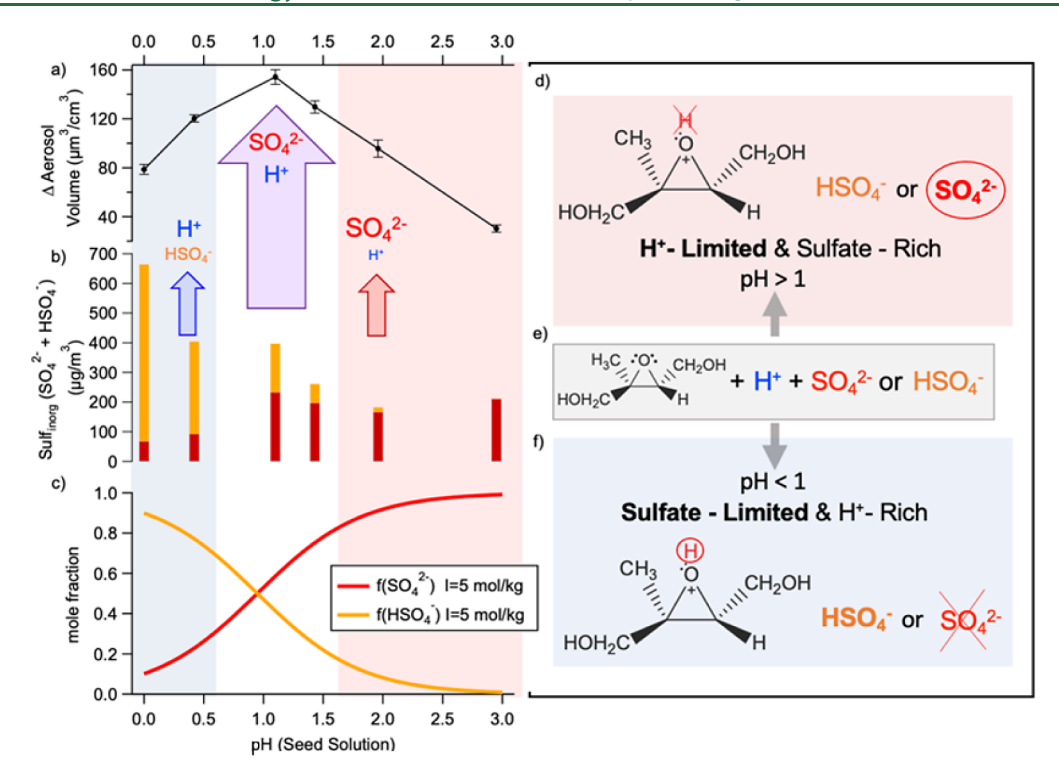


Figure 1. a)  $\Delta$ Aerosol volume at maximum for SOA formed at each seed pH solution value. Error represents 95% confidence interval in the sigmoid fit of raw SEMS volume data. b) Mass concentration of Sulf<sub>inorg</sub> in seed particles as sulfate (red) and bisulfate (yellow). Mass fraction is predicted based on p $K_a$  of species under high ionic strength conditions comparable to that in aerosol particles. c) Mole fraction of sulfate and bisulfate at ionic strength I = 5 mol/kg (see details in the Supporting Information). Shaded regions represent the SO<sub>4</sub><sup>2-</sup>-limited regime (blue) and the H<sup>+</sup>-limited regime (red). Region without shading represents maximum SOA growth. (d-f) Schematic depicting reactants that contribute to the formation of SOA in the two regimes: "H<sup>+</sup>-limited and sulfate-rich" and "sulfate-limited and H<sup>+</sup>-rich".

partition to the particle phase, increasing aerosol mass.<sup>21,22</sup> The observation that epoxides are high yield products from oxidation of isoprene under low-NO conditions, particularly isoprene epoxydiols (IEPOX), 23,24 means that the acidity of atmospheric aerosols is critical due to pH-dependent epoxide ring-opening reactions with nucleophilic species, including sulfate (SO<sub>4</sub><sup>2-</sup>) and water (H<sub>2</sub>O) in the particle phase, forming low-volatility particle phase reaction products such as organo-sulfates and polyols, <sup>6,12,22,25,26</sup> respectively. Field and laboratory measurements have demonstrated that IEPOX undergoes acid-driven reactive uptake onto existing inorganic sulfate particles, leading to substantial formation of methyltetrol sulfates (MTSs) and 2-methyltetrols (2-MTs), up to 15% and 5% of ambient SOA, respectively.<sup>27–30</sup> The formation of MTSs in aerosols has been previously shown to depend on both aerosol acidity<sup>5-7,26</sup> and sulfate concentration,<sup>31</sup> with MTS formation higher at low pH and at higher sulfate concentration.

Both inorganic sulfate species (Sulf<sub>inorg</sub> =  $SO_4^{2-} + HSO_4^-$ ) can act as nucleophiles, but recent laboratory studies by Aoki et al.<sup>32</sup> found that the nucleophilicity of sulfate is  $100 \times$  greater than that of bisulfate ( $HSO_4^-$ ) for epoxides representative of SOA. As pH decreases below the p $K_a$  of sulfate/bisulfate (i.e.,  $pK_{a2}$  of sulfuric acid), bisulfate becomes the dominant form of Sulf<sub>inorg</sub>. While models currently in use predict that MTS formation will increase as pH decreases, it has been unclear how the equilibrium shift from sulfate to bisulfate under low pH conditions will impact the formation of SOA and product distribution of organosulfates versus polyols. In this study, we investigated the formation of IEPOX-derived SOA on acidic aqueous particles ( $H_2SO_4 + (NH_4)_2SO_4$ ) with initial pH values

ranging from 0 to 3 using chamber studies. Atmospheric aerosol particles are highly nonideal and consist of very high ionic strengths,  $^{4,33-36}$  influencing physical properties including the dissociation constant of sulfate/bisulfate.  $^{37-39}$  We use the Dickson equations  $^{37}$  to predict the fraction of sulfate and bisulfate under nonideal conditions relevant to SOA particles and show that at low aerosol pH values (pH < 1) the concentration of bisulfate greatly exceeds sulfate after accounting for ionic strength. Aerosol volume growth due to SOA formation is greatest at pH 1, the most acidic pH where appreciable sulfate is still present. The conversion of Sulf<sub>inorg</sub> to organic sulfate (Sulf<sub>org</sub>), as sulfate ions are incorporated into organosulfate molecules, also had a maximum at pH 1, as determined independently via ion chromatography (IC).

The shifting product distribution (MTSs and 2-MTs) was determined using hydrophilic interaction liquid chromatography coupled with electrospray ionization high-resolution quadrupole time-of-flight mass spectrometry (HILIC/ESI-HR-QTOFMS) operated in the negative ion mode. We find that the branching ratio of MTSs to 2-MTs decreases with increased acidity, indicating a shift from nonvolatile MTS species that do not partition to the gas phase to the semivolatile, nonsulfate-containing 2-MT species, which could help explain a missing source of 2-MTs in models. 40,41 A decreased branching ratio is predicted to occur as water, the necessary nucleophile for 2-MT formation, 42 is still present in abundance and not impacted by the sulfate/bisulfate equilibrium. Our results indicate that maximal SOA growth will occur on particles at pH 1, and that particles with very high acidity (pH < 1) will result in less SOA mass. Modeling of SOA formation and speciation based on the widely used

parameterization from Eddingsaas et al.  $^{42}$  indicates that this underappreciated sulfate-limitation could lead to overpredictions of SOA mass resulting from the formation of organosulfates in regions with high aerosol acidity (pH < 1).

#### MATERIALS AND METHODS

No unexpected or unusually high safety hazards were encountered.

**Aerosol Generation.** SOA was generated from the reactive uptake of trans-β-IEPOX, which is the most atmospherically abundant isomer of IEPOX.<sup>24</sup> The synthesized trans-β-IEPOX standard was prepared using previously described procedures.<sup>5,43</sup> The atmospheric chamber experiments were conducted following the previously published methods<sup>5,12,44-46</sup> at the University of North Carolina at Chapel Hill (UNC) 10-m<sup>3</sup> indoor chamber facility operated under dark conditions. All of the chamber experiments were conducted at the same relative humidity (RH) (i.e., 50% RH). Aerosol particles were generated from solutions of ammonium sulfate (Sigma-Aldrich, ≥99% purity), sulfuric acid (Sigma-Aldrich, ≥98% purity), and Milli-Q water (17.8 MQ cm<sup>-1</sup>). The solutions were acidified with sulfuric acid to the target pH and measured with a pH probe (Hanna Instruments). The seed solution conditions for each experiment are described in Tables S1 and S2. The total  $Sulf_{inorg}$ , which includes both  $SO_4^{\ 2-}$  and  $HSO_4^{\ -}$ , in the seed aerosol was maintained constant at 0.12 M for the pH 1-3 experiments, based on prior work,  $^{5,45}$  and the Sulf<sub>inorg</sub> value was increased to achieve lower pH conditions (0.5 M, pH 0.4; 1 M, pH 0). The seed solutions were aerosolized into the chamber using a custom-built atomizer at a flow rate of 5 L min<sup>-1</sup> to reach a volume concentration of  $160-200 \, \mu \text{m}^3/\text{cm}^3$ . Note that slight differences in the starting volume concentration of the seed particles is reflected in the initial [Sulf<sub>inorg</sub>] reported in Figure 1b. After the seed concentration stabilized, gaseous trans- $\beta$ -IEPOX was introduced into the chamber through a heated manifold (~60 °C) with high-purity nitrogen gas and injected at 2 L min<sup>-1</sup> for 10 min, and then 5 L min<sup>-1</sup> for 50 min, totaling 60 min of IEPOX injection, based on previous studies. 5,12,46 Afterward, aerosol particles reacted in the chamber for 60 min without any additional IEPOX being added. The aerosol size distributions for the experiments listed in Table S1 are shown in Figure S1 for the seed particles and SOA particles generated after 1 h of reaction in the chamber, which represents the time point at which IEPOX injection was stopped. The size distributions confirm that increasing sulfate concentration for the experiments at pH 0 and 0.4 does not significantly increase the size mode of the seed particles.

Aerosol pH. It should be noted that the aerosol pH values noted herein represent bulk pH value measurements of the seed solution. We recognize that there are likely differences between the bulk solution and aerosol pH values based on previous measurements,<sup>47</sup> but we were unable to obtain measurements of the aerosol pH in the chamber due to insufficient aerosol liquid water content, the range of the pH paper, and the potential for pH to change during the experiment. The listed bulk pH for the experiments included herein should be considered as an upper bound of aerosol pH (i.e., the aerosol pH is likely lower than the bulk values reported in this manuscript).

Additionally, we would like to note that it is likely that the aerosol pH changes over the course of the experiment as water is consumed in the nucleophilic addition to IEPOX to form

methyltrols and as the more hygroscopic inorganic sulfate fraction is converted into a less hygroscopic organic fraction (i.e., organosulfates like MTSs). In addition, it is possible that the change in aerosol pH is influenced by a number of factors (i.e., starting [Sulf]<sub>inorg</sub>, seed composition, IEPOX injected, aerosol morphology, and aerosol fraction of organosulfates). Future studies are needed to comprehensively characterize changes in aerosol pH over the course of a chamber experiment.

**Aerosol Measurements.** It should be noted that the measurements reported in this study are not wall-loss corrected. Based on previous experiments conducted using this chamber, 5,46 we do not expect a significant difference in wall loss between the experiments conducted in this study and do not expect that the rate of wall loss will change the conclusions discussed herein.

The aerosol particle volume was measured with a scanning electron mobility spectrometer (SEMS, BMI Inc., Model 2100),  $^{48}$  which consists of a differential mobility analyzer (DMA, BMI model 2002) and a mixing condensation particle counter (MCPC, BMI model 1710) that measures aerosol at a time resolution of 80 s. After entering the SEMS, the sample air flow was combined with a sheath flow with a RH lower than that in the chamber, which results in a decrease in the RH compared to that of the chamber (range of  $\sim\!25-35\%$  at bottom of column). The SEMS system monitors aerosol number concentrations, dry bulk aerosol size distribution, and dry volume concentration. The change in aerosol volume was calculated by comparing the maximum aerosol volume formed in each experiment to the initial aerosol volume before IEPOX injection eq 1.

$$\Delta$$
Aerosol Volume = Volume at Maximum

- Initial Aerosol Volume (1)

It should be noted that SOA growth is reported herein as  $\Delta$ volume and is not converted to SOA mass formation. This is due to the uncertainties associated with the density of the particles, which likely changes significantly over the course of the experiment as inorganic sulfate is converted to organosulfate species. Future studies should conduct in situ density measurements of SOA formed from the reactive uptake of IEPOX onto inorganic sulfate seed particles.

Throughout the chamber experiments, aerosol particles were collected using a particle-into-liquid sampler (PILS, BMI model 4001) for quantification of inorganic sulfate using IC, and quantification of MTSs and 2-MTs using HILIC/ESI-HR-QTOFMS operated in the negative ion mode. While we recognize that additional products may form within IEPOX-SOA (e.g., oligomers, including sulfated oligomers, as well as IEPOX isomerization products), our analysis focuses on the quantification of MTSs and 2-MTs based on the availability of authentic standards. Additionally, the PILS samples were unfortunately too dilute for HILIC/ESI-HR-QTOFMS analysis to investigate organosulfate oligomers that would be formed in much lower concentrations.

IC was used to determine the conversion of inorganic sulfate in the initial particles to organosulfates in the particles after the IEPOX reaction throughout the chamber experiment. Darer et al.  $^{49}$  previously reported that the lifetime of MTS species against acid-catalyzed hydrolysis is  $\sim\!60$  h, even under pH 0 conditions. Thus, IC analysis was completed within 10 h of completion of the chamber experiment to prevent sample

degradation, particularly hydrolysis of MTS species. A 25- $\mu$ L aliquot of the PILS sample was analyzed using an anion exchange IC (ICS 3000, ThermoFisher) with a conductivity detector (Dionex, run at 35 °C). The instrument contains an IonPac AS11-HC guard column (2 × 50 mm ThermoFisher) and an anion-exchange column (2 × 250 mm ThermoFisher) run at a flow rate of 0.4 L min<sup>-1</sup>. The elution gradient and product assignment of chromatographic peaks are as described previously. The technique was applied to quantify the mass of inorganic sulfate within the PILS samples, and the % inorganic sulfate conversion was calculated by comparing the mass of inorganic sulfate in the SOA to that of the sulfate seed particles eq 2.

% Inorganic Sulfate Conversion at time

$$= x(t_x)$$
= Mass Sulf<sub>inorg(t\_y)</sub> - Mass Sulf<sub>inorg(t\_0)</sub> (2)

HILIC/ESI-HR-QTOFMS was used to quantify the MTS and 2-MT products in the SOA particles. Shortly after collection, a 50-µL aliquot of each PILS aqueous sample was diluted in 950  $\mu$ L of acetonitrile (ACN, HPLC grade, Fischer Scientific) in order to achieve the solvent composition of the HILIC mobile phase (i.e., 95:5 ACN:H<sub>2</sub>O). The diluted PILS samples were stored in the dark at −20 °C prior to analysis. All samples were analyzed within 2 weeks and most analyzed within a week or less to prevent any sample degradation from occurring (i.e., hydrolysis of MTS species). HILIC/ESI-HR-QTFOMS was conducted as described previously<sup>27,50</sup> with an Agilent 6520 Series Accurate Mass Q-TOFMS with an ESI source operated in negative ion mode coupled to an Agilent 6500 Series UPLC equipped with a Waters ACQUITY UPLC BEH Amide column. The HILIC/ESI-QTOFMS operating conditions, including the elution gradient program, mass calibration, tuning, and voltages, were as previously described.<sup>50</sup> Error for MTS and 2-MT quantification was represented as % relative standard error for the HILIC/ESI-HR-QTOFMS method as described by Cui et al.<sup>27</sup>

IEPOX Injection Control Experiments. It has previously been established that the mass of IEPOX injected during an experiment influences the amount of SOA formation, with increased IEPOX:SO<sub>4</sub><sup>2-</sup> ratios resulting in greater organosulfate formation. We compare the formation of SOA as a function of IEPOX mass injected. We find that the greatest amount of aerosol volume formation occurs at pH 1 over a wide range of IEPOX mass injected (1.9–11.6 mg). Specifically, we compare SOA volume formation (Figure S2), inorganic sulfate consumption, and MTS/2-MT mass formed (Figure S3), as well as the branching ratio (Figure S6), as a function of IEPOX mass injected for experiments conducted at pH 0–5. These results confirm that the shift from sulfate to bisulfate with decreasing pH is a key factor to predict the amount of SOA formation.

**Aerosol Modeling.** The extended aerosol inorganics model III (E-AIM) was used to predict the chemical composition and ionic strength of the aerosol particles. The bulk solution conditions (Table S1) for the ammonium sulfate seed solution were used as the starting ionic composition, and a fixed RH of 50% was assumed. Based on the RH conditions of the chamber, all solids were prevented from forming in the thermodynamic model. The input and output for each experiment are provided (Tables S4–S10). The Eddingsaas equations were used to predict the SOA

yield that formed based on the bulk solution composition. A detailed description of the application of the Eddingsaas parameterization is discussed in the Supporting Information.

## ■ RESULTS AND DISCUSSION

Impact of Acidity on Aerosol Growth. To determine the effect of initial particle acidity on SOA formation, particles were generated by nebulizing seed solutions of different pH values into a dark 10-m<sup>3</sup> atmospheric simulation chamber. Seed particles were mixtures of ammonium sulfate and sulfuric acid nebulized from solutions with pH values ranging from 0 to 3, representative of common fine atmospheric aerosol acidities.<sup>4,14</sup> Synthesized trans-β-IEPOX,<sup>43</sup> the predominant atmospheric IEPOX isomer,<sup>24</sup> was injected into the chamber where it reacted with the acidic particles. The amount of SOA formed was determined by the increase in aerosol volume after IEPOX injection (Figure 1a). While maintaining Sulfinorg concentrations constant (0.12 M) and decreasing the pH from ~3 to 1 (2.95, 1.96, 1.43, and 1.10), the amount of SOA formed increased, showing pH-dependent SOA formation independent of total Sulf<sub>inorg</sub>. For more acidic solutions (pH 0.42 and 0.0), greater  $Sulf_{inorg}$  concentrations were necessary to reach these pH values ( $Sulf_{inorg} = 0.5$  and 1.0 M, respectively). Notably, maximum SOA formation was observed at pH 1.10, and less SOA formed for more acidic solutions (pH values of 0.0 and 0.42) despite the presence of greater [H+] and [Sulf<sub>inorg</sub>]. The SOA formation maximum at pH  $\sim$  1 was confirmed with replicate experiments across the pH range (Figure S2 and Tables S1 and 2). These results show that SOA formation does not monotonically increase for epoxides with decreasing pH (increasing acidity) or increasing Sulfinorg.

Maximal aerosol volume growth from IEPOX reactive uptake (Figure 1a) is dependent upon nucleophilic attack by SO<sub>4</sub><sup>2-</sup> and H<sub>2</sub>O under acidic conditions. The aerosol concentration of [H<sup>+</sup>] to protonate the epoxide depends on the aerosol pH, as does the concentration of  $SO_4^{2-}$ , one of two key nucleophiles. At pH values below the pK<sub>a</sub> for sulfate/ bisulfate ( $pK_a = 2$  under dilute conditions), bisulfate, the weaker nucleophile, is the dominant form of Sulf<sub>inorg</sub>, thus reducing the amount of particulate MTS formation. Further complicating matters, aerosol particles can reach very high ionic strengths (I) in the atmosphere due to low water contents.<sup>33</sup> Thus, the dissociation constant of sulfate/bisulfate shifts to lower values approaching  $pK_a = 1$  under the high ionic strength (I = 12-46 mol/kg) conditions of the aerosol particles in these experiments (Table S3).37-39 For experiments with pH values below this shifted p $K_a$  value (pH < 1), most Sulf<sub>inorg</sub> is bisulfate (77% at pH 0.4 and 90% at pH 0, Figures 1b,c). Thus, the moles of  $SO_4^{2-}$  available for nucleophilic addition decrease as the sulfate equilibrium shifts to predominantly bisulfate (Figure 1c), despite moles of H<sup>+</sup> dramatically increasing at lower pH (pH < 1). In contrast, at higher pH ranges (pH > 1),  $Sulf_{inorg}$  is dominated by  $SO_4^{2-}$  (minimal  $HSO_4^{-}$ ), but  $H^+$  is limited. Thus, pH 1 represents the optimal concentration of both reactants (H<sup>+</sup> and SO<sub>4</sub><sup>2-</sup>) to form low-volatility particulate organosulfates, which matches with the maximum SOA volume formed as shown in Figure 1a. The details of the seed solution composition and pH, as well as ionic strength calculations and the dissociation constant shift are discussed in the Tables S1-S3, respectively. Hereafter, we refer to three different pH ranges as "H+-limited and sulfaterich" regime at pH values above the shifted pK<sub>a</sub> of sulfate/ bisulfate (i.e., pH > 1.5), "maximum SOA formation" regime

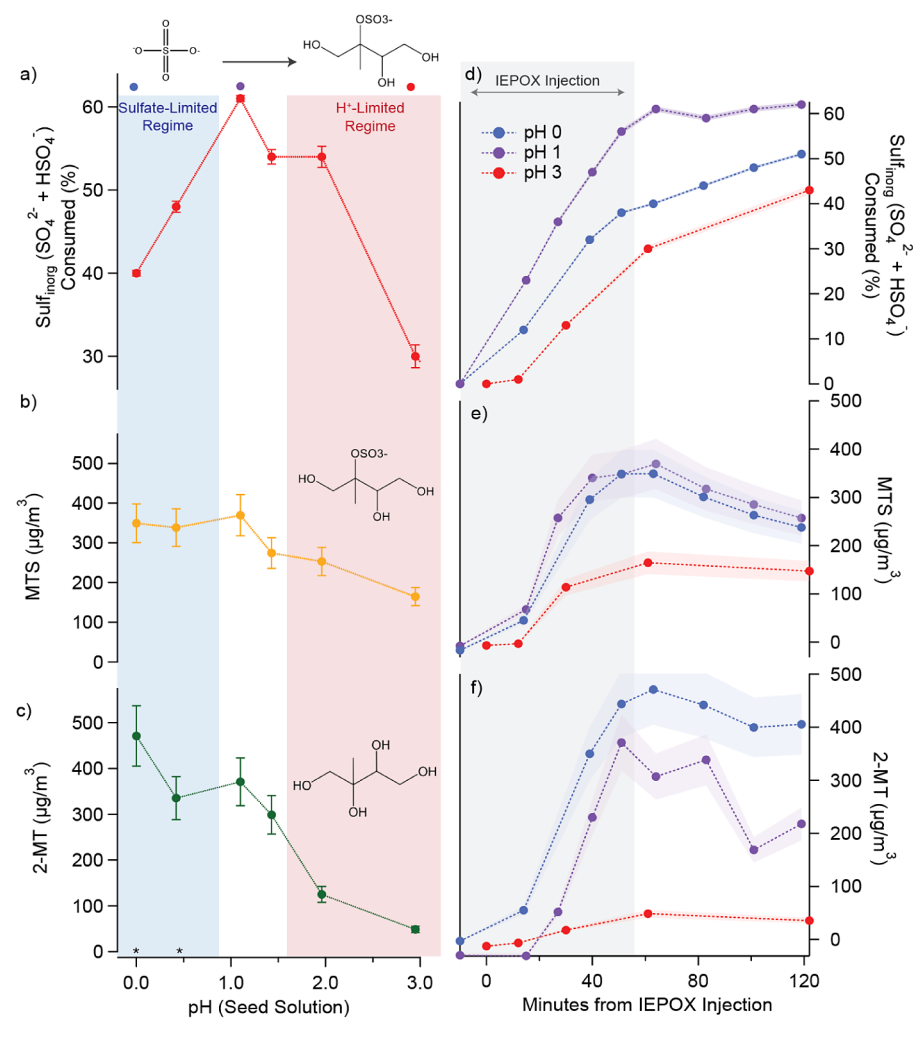


Figure 2. a) The % inorganic sulfate remaining at 60 min of IEPOX reaction, b) maximum mass concentration of MTSs formed, and c) maximum mass concentration of MT formed (bottom) at different solution pH values. Error bars represent % relative standard error. Shaded regions represent SO<sub>4</sub><sup>2-</sup>-limited regime (blue) and H<sup>+</sup>-limited regime (red). Unshaded region represents pH values with maximum SOA formation. Asterisks indicate experiments with increased [Sulf<sub>inorg</sub>] to achieve that pH. Graphical illustration of measurement is shown, including the conversion of inorganic to organosulfate (2a), quantification of MTS species (2b), and quantification of 2-MT species (3b). Comparison of time-resolved d) % inorganic sulfate remaining; e) MTS mass concentration over time, the shaded region represents % relative standard error; and f) MT mass concentration, the shaded region represents % relative standard error. The gray shaded region indicates 60 min of continuous IEPOX injection into the atmospheric chamber. Afterward, the particles were reacted for 1 h without any additional IEPOX. Three experiments shown represent the three regions: SO<sub>4</sub><sup>2-</sup> limited regime (pH 0, blue), H<sup>+</sup> limited regime (pH 3, red), and regime of maximum SOA formation (pH 1, purple).

at  $\sim$ pH 1–1.5, and "sulfate-limited and H<sup>+</sup>-rich" regime at pH values below the shifted p $K_a$  of sulfate/bisulfate (i.e., pH < 1) (Figure 1d–f). Overall, aerosol pH at  $\sim$ 1 produces maximal SOA growth (across more than 20 experiments shown in Tables S1 and S2), as it is the most acidic condition with sufficient SO<sub>4</sub><sup>2–</sup> present to form low-volatility organosulfates in the particles.

Impact of Acidity on Organosulfate Formation. To confirm the impact of seed solution pH on organosulfate formation, we used IC to quantify the amount of inorganic sulfate consumed during organosulfate formation in the atmospheric simulation chamber after 60 min of reaction (Figures 2a and S3a); it is noted that these conversions are much faster than aerosol loss to chamber walls can explain, and is consistent with prior studies. Sulf<sub>inorg</sub> to organosulfate conversion increased as a function of decreasing pH for less acidic conditions (2.95, 1.96, 1.43, and 1.10), indicating that

particle acidity increased the formation of organosulfate species. However, the greatest  $Sulf_{inorg}$  to organosulfate conversion occurred in particles at seed solution pH 1 (~60%), which provides independent confirmation of the maximum SOA volume growth as shown in Figure 1a. For the more acidic experiments (below pH of 1),  $Sulf_{inorg}$  conversion decreased (~50% at pH of 0.42 and only 40% at pH of 0.0), despite higher initial [ $Sulf_{inorg}$ ] needed to achieve these lower pH conditions. These results show that incorporation of  $Sulf_{inorg}$  into organosulfate molecules does not continue to increase as the sulfate-bisulfate equilibrium shifts to bisulfate below the p $K_s$ .

The mass concentration of the key organosulfate product (MTS) was quantified with HILIC/ESI-HR-QTOFMS, as well as 2-MTs (formed from  $\rm H_2O$  as the nucleophile), as a function of pH (Figure 2b,c and Figure S3b,c). MTS formation increased as seed solution pH decreased from 2.95 to 1.95

to 1.4 to 1, agreeing with previous research indicating that MTS formation increases with increased particle acidity.<sup>2</sup> However, below pH 1, greater MTS formation was not observed at pH 0.4 or 0.0, which agrees with less SOA volume formed and less Sulf<sub>inorg</sub> consumed. It is notable that MTS formation no longer increases for the seed solutions at pH 0.0 and 0.4, as we had to use higher initial [Sulf<sub>inorg</sub>] to reach the lower pH values, which hypothetically could have facilitated greater MTS formation. 46 In contrast, 2-MT formation peaked for the lowest pH used (pH 0.0). Unlike sulfate, which is limited below the pH of the dissociation constant, H<sub>2</sub>O availability for nucleophilic addition is not limited with decreasing pH and will not change under these highly acidic conditions. In addition, 2-MTs are much more volatile than MTSs, 55,56 which means that a substantial fraction of 2-MTs may have partitioned to the gas phase after formation. The evaporation rate of semivolatile species increases under more acidic conditions,<sup>57</sup> which could mean that 2-MTs formed under these highly acidic conditions could volatilize from the particles, subsequently decreasing the aerosol volume. Our measurements quantified particulate 2-MTs, and future work should quantify the overall 2-MT yield (gas + particle) as a function of pH to investigate whether a greater amount of 2-MTs is formed and subsequently volatilizing under these highly acidic conditions. Additionally, it is possible that the formation of additional species beyond MTSs and 2-MTs, particularly those that can partition to the gas-phase after inparticle formation such as C<sub>5</sub>-alkene triols, 10 could further explain the decreased SOA formation below pH 1, and future experiments should probe the composition of gas-phase species as a function of seed aerosol pH. Taken together, the three independent measures of SOA production (i.e., aerosol volume growth from SEMS, inorganic sulfate consumption from IC, and MTS/2-MT formation from HILIC-ESI-HR-QTOFMS) all point to a maximum in SOA production and organosulfate formation at pH ~1, with less SOA and organosulfate formation at pH 0 and 0.4, which demonstrates that under the most acidic conditions IEPOX-derived SOA formation depends on more than acidity and [Sulf<sub>inorg</sub>].

Time-Resolved SOA Formation. To gain insight into the time-dependent dynamics of SOA formation, we compared the aerosol volume growth, Sulfinorg consumption, and MTS/2-MT formation for the three regimes studied (i.e., maximum SOA formation at pH 1, SO<sub>4</sub><sup>2-</sup>-limited regime at pH 0, and H<sup>+</sup>limited regime at pH 3) in Figures 2d-f, respectively (experiments at other pH values in Figure S4). The greatest increase in Sulfinorg consumption occurred at pH 1, which stopped increasing at 60 min once IEPOX injection ceased, indicating rapid kinetics of IEPOX conversion to organosulfates. Under both pH 0 and 3 conditions, sulfate consumption continued after IEPOX injection ended, indicating that equilibrium was not reached during the first 60 min of reaction due to slower kinetics for SOA formation. The time-resolved formation of particulate MTSs and 2-MTs each reached a maximum at ~60 min of reaction time in each regime: pH 0, 1, 3 (Figure 2e,f). It is possible that aerosol pH changes over the course of the chamber experiment, which could result in the SOA conditions shifting from the "maximum SOA formation" to a "limited" regime, or vice versa. The dynamics of aerosol pH throughout a chamber experiment is currently unknown, and future studies should be conducted focusing on characterizing changes in aerosol pH after the reactive uptake of IEPOX to sulfate aerosol particles.

The reaction for the conversion of MTS products into oligomers is pH-dependent and is enhanced under acidic conditions. Given that the % inorganic sulfate consumption at pH 1 exceeds that of the pH 0 particles while the MTS formation appears comparable, it is possible that the MTS products in the pH 1 experiment are converted into other organosulfate products, such as higher mass oligomeric species. Future studies should characterize the formation of oligomers under highly acidic conditions, especially once authentic standards are available for these compounds, to determine the impact of decreased MTS formation on the formation of higher mass products.

**Sulfate-Limited vs H** $^+$ -**limited Regimes.** To further investigate the time-dependent formation of IEPOX-derived SOA, we compare time-resolved aerosol volume formation for experiments with pH 0–3 (Figure 3). We observed that at pH

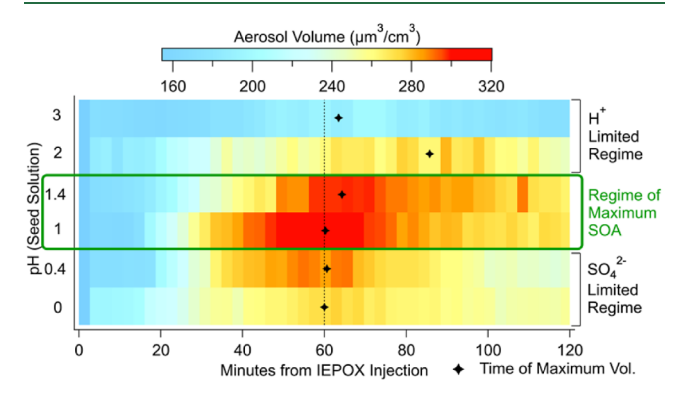


**Figure 3.** Time-resolved aerosol volume ( $\mu$ m³/cm³) for each experiment. IEPOX was injected continuously from 0 to 60 min, and the vertical dashed line represents the point at which IEPOX injection ended. The reaction was monitored from 60 to 120 min with no additional IEPOX added. Black diamonds indicate the time point at which the maximum aerosol volume occurred during the chamber experiment.

1 the aerosol volume quickly increased and reached a maximum at  ${\sim}60$  min. After 60 min, the aerosol volume stabilized until slightly decreasing due to aerosol loss to chamber walls. For a seed solution with a pH <1, the aerosol volume also peaked when IEPOX injection ended. At pH <1, bisulfate is much greater than sulfate, so the reaction will be sulfate-limited, and any sulfate ion present will be quickly depleted. This suggests that  $\left[SO_4^{\ 2^-}\right]$  is a limiting factor in the nucleophilic addition of IEPOX to form MTSs (and potentially other organosulfates) at low pH, consistent with the findings of Xu et al.  $^{31}$ 

Under less acidic conditions (pH 2 and 3), the maximum for aerosol volume was reached later in the reaction at ~86 min and ~64 min, respectively, agreeing with the slower kinetics of sulfate consumption observed in Figure 2d and consistent with prior kinetic studies. This can be explained by the fact that some of the available [H $^{+}$ ] is initially consumed as IEPOX undergoes reactive uptake. However, more [H $^{+}$ ] can form from Le Chatelier's principle pushing the autoionization of water (H<sub>2</sub>O  $\leftrightarrow$  H $^{+}$  + OH $^{-}$ ) equilibrium toward H $^{+}$  and OH $^{-}$ . The newly formed H $^{+}$  then protonates any remaining IEPOX allowing the remaining [SO<sub>4</sub> $^{2-}$ ] to nucleophilically attack and form organosulfates, even after IEPOX injection ended. Overall, pH 1 represents the optimum balance of [H $^{+}$ ] and [SO<sub>4</sub> $^{2-}$ ], which results in maximal SOA formation.

Modeling SOA Formation as a Function of Aerosol Acidity. To predict SOA yield, many current atmospheric models, including GAMMA (Gas-Aerosol Model for Mechanism Analysis), <sup>59</sup> GEOS-Chem (Goddard Earth Observing System-Chemistry), <sup>60</sup> and the CMAQ (Community Multiscale Air Quality) model, <sup>61</sup> use rate constants determined from a study conducted in 2010 by Eddingsaas et al. <sup>42</sup> in which beaker-scale experiments (bulk) were conducted using epoxybutanol and epoxy-butanediol as proxies for IEPOX. We generate the predicted SOA yield from our atmospheric chamber experiments based on the Eddingsaas equations, the details of which are described in the Supporting Information. Comparing our experimental results to the output (Figure 4a)

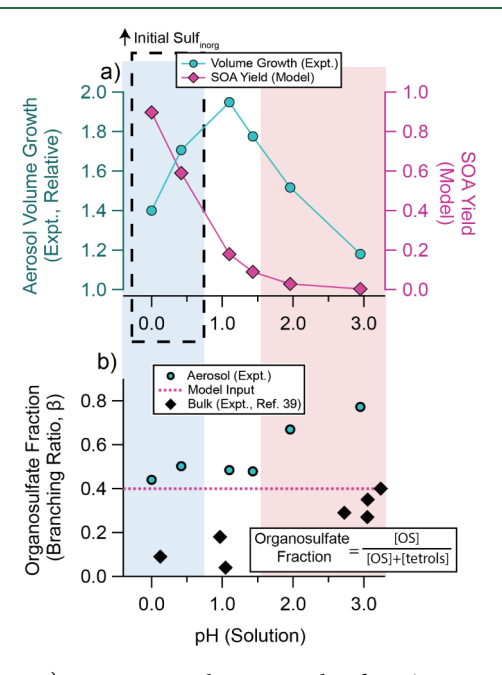


Figure 4. a) Maximum volume growth after 60 min reaction normalized to the initial volume at t=0 in the chamber experiments using SEMS compared to SOA yield predicted using the Eddingsaas rate equations b) organosulfate fraction or "branching ratio" ( $\beta$ ) for MTSs and 2-MTs after ~50 min reaction with IEPOX based on timeresolved  $\beta$  including in Figure S6. The dashed line indicates the  $\beta$  determined by Eddingsaas et al. ( $\beta$  = 0.4) that is commonly used as a model input. The inset is the formula used to calculate the organosulfate fraction. For ref<sup>39</sup>, the branching ratio was calculated comparing the fraction of sulfate esters to tetrols.

demonstrates that atmospheric models likely overpredict the amount of SOA and MTSs forming at pH values below 1. The SOA yield based on the Eddingsaas equations predicts that SOA production will increase significantly as pH decreases, particularly below pH 1, reaching yields up to 90% at pH 0. Our results indicate that the pH-dependent formation of IEPOX-derived SOA needs to be updated in models in order to accurately predict the amount of SOA formation through this reaction pathway. Our experimental measurements of the mass concentration of particulate MTSs and 2-MTs formed based on aerosol pH are compared with modeled MTS and 2-MT formation (Figure S5), which shows less formation than the model parametrization predicts in the sulfate-limited regime (pH < 1). The HILIC/ESI-HR-QTOFMS mass concentrations also show greater MTSs and 2-MTs at pH >1 compared to the model, including formation at pH values of 2 and 3 even though the model predicts minimal SOA

formation at those pH's. These findings can help improve predictions of IEPOX-derived SOA and organosulfate formation over a broader pH range representative of more locations.<sup>4</sup>

To determine the relative fractions of MTSs and 2-MTs formed, many current models use a branching ratio  $(\beta)$  that parameterizes the SOA yield into the MTS and 2-MT products.<sup>59</sup> The branching ratio is typically prescribed from the Eddingsaas aqueous IEPOX chemistry parameters from beaker-scale experiments (bulk) conducted using proxies for IEPOX. 42 These bulk studies showed the  $\beta$  of sulfate esters and tetrols ranges from 0.09 to 0.4 as a function of acidity (pH  $\sim 0-3$ ) and sulfate concentration (0.1–3.1 M). Currently, models apply  $\beta$  from the bulk value with the highest sulfate concentration ( $\beta = 0.4$ ) to predict the relative amounts of particulate organosulfates versus tetrols in SOA.<sup>59</sup> We compare the  $\beta$  from aerosol particles (this study) to the bulk solution experiments and find that  $\beta$  is greater in the aerosol phase across the entire pH range (Figure 4b). Additionally, the relative amounts of organosulfates versus tetrols increase substantially with pH, reaching 77% at pH 3. This higher organosulfate formation in relation to polyols in suspended particles, in contrast to beaker-based experiments, is important to consider for future predictions of IEPOX-derived SOA formation, given the much lower volatility of organosulfates versus polyols (e.g., 2-MTs). 55,56 Additionally, the increase in 2-MTs at lower pH and subsequent volatilization could help explain the missing pathway for 2-MTs identified in recent studies where 20-40% of 2-MTs could not be explained using current models, 40 particularly if the 2-MT partitions back to the condensed phase in the free troposphere at lower temperatures.

Overall, we show that accurately predicting isoprene-derived SOA mass requires accounting for aerosol acidity, acid dissociation constants, and ionic strength. The experiments above show that SOA formation does not increase monotonically as aerosol pH decreases (acidity increases), instead observing the highest SOA formation at pH = 1. Below pH = 1(ionic strength-shifted pK<sub>a</sub>), when bisulfate is the dominant species of [Sulf<sub>inorg</sub>], the aerosol volume of IEPOX-SOA decreases. This lower SOA formation under the lowest pH conditions in our experimental results is not captured by current models, leading to overpredictions of SOA formation under the most acidic conditions. This previously unaccounted for maximum in SOA yield shows the importance of considering acid-base equilibria, specifically the sulfatebisulfate equilibrium, when predicting acid-driven heterogeneous chemistry leading to IEPOX-SOA. As atmospheric aerosols are typically very acidic, <sup>4</sup> particularly in the submicron size range where most SOA formation occurs (pH = -0.5-3.0),4,8 accounting for pH-dependent behavior is essential. Accounting for the acid-base equilibrium is important for other acids and their conjugate bases within ambient aerosols (nitric acid, nitrate, and carboxylic acids) and accounting for this equilibrium behavior will improve predictions of PM<sub>2.5</sub> concentrations and guide mitigation actions to improve human health.

# ASSOCIATED CONTENT

# **Solution** Supporting Information

The Supporting Information is available free of charge at https://pubs.acs.org/doi/10.1021/acs.est.3c10851.

Additional information including aerosol size distributions (Figure S1); aerosol volume growth as a function of [IEPOX] and starting pH (Figure S2); experimental details for main text (Table S1) and supplemental text (Table S2) figures; ionic strength calculation (eq S1); model predictions of bulk and single particle ionic strength (Table S3); input values for E-AIM model III (Table S4); results from E-AIM model for bulk pH 3 (Table S5), pH 2 (Table S6), pH 1.5 (Table S7), pH 1 (Table S8), pH 0.5 (Table S9), and pH 0 (Table S10); summary of chamber experiment results (Table S11); inorganic sulfate consumption, MTS formation, and 2-MT formation as a function of [IEPOX] and starting pH (Figure S3); time-resolved volume formation, inorganic sulfate consumption, MTS formation, and 2-MT formation (Figure S4); speciated product yield vs model (Figure S5); branching ratio calculation (eq S2); pH-dependent branching ratio (Figure S6); and SOA yield calculations (eqs S3–S6) (PDF)

### AUTHOR INFORMATION

# **Corresponding Authors**

Jason D. Surratt — Department of Environmental Sciences and Engineering, Gillings School of Global Public Health, University of North Carolina at Chapel Hill, Chapel Hill, North Carolina 27516, United States; Department of Chemistry, College of Arts and Sciences, University of North Carolina at Chapel Hill, Chapel Hill, North Carolina 27599, United States; orcid.org/0000-0002-6833-1450; Email: surratt@unc.edu

Andrew P. Ault — Department of Chemistry, University of Michigan, Ann Arbor, Michigan 48109, United States; orcid.org/0000-0002-7313-8559; Email: aulta@umich.edu

# **Authors**

Madeline E. Cooke – Department of Chemistry, University of Michigan, Ann Arbor, Michigan 48109, United States

N. Cazimir Armstrong — Department of Environmental Sciences and Engineering, Gillings School of Global Public Health, University of North Carolina at Chapel Hill, Chapel Hill, North Carolina 27516, United States

Alison M. Fankhauser — Department of Chemistry, University of Michigan, Ann Arbor, Michigan 48109, United States;
orcid.org/0000-0002-8303-8308

Yuzhi Chen — Department of Environmental Sciences and Engineering, Gillings School of Global Public Health, University of North Carolina at Chapel Hill, Chapel Hill, North Carolina 27516, United States; orcid.org/0000-0002-2547-8428

Ziying Lei — Department of Environmental Health Sciences, University of Michigan, Ann Arbor, Michigan 48109, United States; Present Address: Department of Atmospheric Sciences, Texas A&M University, College Station, Texas, United States 77843

Yue Zhang — Department of Environmental Sciences and Engineering, Gillings School of Global Public Health, University of North Carolina at Chapel Hill, Chapel Hill, North Carolina 27516, United States; Present Address: Department of Atmospheric Sciences, Texas A&M University, College Station, Texas, United States 77843; orcid.org/0000-0001-7234-9672

Isabel R. Ledsky – Department of Chemistry, Carleton College, Northfield, Minnesota 55057, United States

Barbara J. Turpin — Department of Environmental Sciences and Engineering, Gillings School of Global Public Health, University of North Carolina at Chapel Hill, Chapel Hill, North Carolina 27516, United States; orcid.org/0000-0003-4513-4187

**Zhenfa Zhang** — Department of Environmental Sciences and Engineering, Gillings School of Global Public Health, University of North Carolina at Chapel Hill, Chapel Hill, North Carolina 27516, United States

Avram Gold — Department of Environmental Sciences and Engineering, Gillings School of Global Public Health, University of North Carolina at Chapel Hill, Chapel Hill, North Carolina 27516, United States; orcid.org/0000-0003-1383-6635

V. Faye McNeill — Department of Chemical Engineering, Columbia University, New York, New York 10027, United States; Occid.org/0000-0003-0379-6916

Complete contact information is available at: https://pubs.acs.org/10.1021/acs.est.3c10851

# **Author Contributions**

<sup>∇</sup>M.E.C. and N.C.A. contributed equally.

#### Notes

The authors declare no competing financial interest.

### ACKNOWLEDGMENTS

This work was supported by the National Science Foundation (NSF) under a CAREER Award CHE-1654149 and grants AGS-1703019 (Ault) and AGS-2040610 (Ault), as well as AGS-1703535 (Surratt) and AGS-2039788 (Surratt). A.G., Z.Z., and J.D.S. also acknowledge support from NSF grant no. AGS-2001027 (Gold, Zhang). M.E.C. was supported by an NSF Graduate Research Fellowship (NSF-GRFP) DGE-1841052. Y.Z. was supported by the NSF Postdoctoral Fellowship under AGS-1524731. HILIC/ESI-HR-QTOFMS work was performed in the UNC Biomarker Mass Spectrometry Facility, which is supported by the National Institute of Environmental Health Sciences (grant number P30ES010126). The Sloan Foundation is also acknowledged for support via grants FG-2018-10226 and G-2018-11239 (Ault).

#### REFERENCES

(1) Pöschl, U. Atmospheric Aerosols: Composition, Transformation, Climate and Health Effects. *Angew. Chem., Int. Ed.* **2005**, 44 (46), 7520–7540.

(2) Wolf, M. J.; Zhang, Y.; Zawadowicz, M. A.; Goodell, M.; Froyd, K.; Freney, E.; Sellegri, K.; Rösch, M.; Cui, T.; Winter, M.; et al. A biogenic secondary organic aerosol source of cirrus ice nucleating particles. *Nat. Commun.* **2020**, *11* (1), 4834.

(3) Davidson, C. I.; Phalen, R. F.; Solomon, P. A. Airborne Particulate Matter and Human Health: A Review. *Aerosol Sci. Technol.* **2005**, 39 (8), 737–749.

(4) Pye, H. O. T.; Nenes, A.; Alexander, B.; Ault, A. P.; Barth, M. C.; Clegg, S. L.; Fahey, K. M.; Hennigan, C. J.; Herrmann, H.; Kanakidou, M.; Kelly, J. T.; Ku, I. T.; McNeill, V. F.; Riemer, N.; Schaefer, T.; Shi, G.; Tilgner, A.; Walker, J. T.; Wang, T.; Weber, R.; Xing, J.; Zaveri, R. A.; Zuend, A. The acidity of atmospheric particles and clouds. *Atmos. Chem. Phys.* **2020**, 20 (8), 4809–4888.

(5) Lei, Z.; Chen, Y.; Zhang, Y.; Cooke, M. E.; Ledsky, I. R.; Armstrong, N. C.; Olson, N. E.; Zhang, Z.; Gold, A.; Surratt, J. D.; Ault, A. P. Initial pH Governs Secondary Organic Aerosol Phase State

- and Morphology after Uptake of Isoprene Epoxydiols (IEPOX). *Environ. Sci. Technol.* **2022**, *56* (15), 10596–10607.
- (6) Surratt, J. D.; Lewandowski, M.; Offenberg, J. H.; Jaoui, M.; Kleindienst, T. E.; Edney, E. O.; Seinfeld, J. H. Effect of Acidity on Secondary Organic Aerosol Formation from Isoprene. *Environ. Sci. Technol.* **2007**, *41* (15), 5363–5369.
- (7) Gaston, C. J.; Riedel, T. P.; Zhang, Z.; Gold, A.; Surratt, J. D.; Thornton, J. A. Reactive Uptake of an Isoprene-Derived Epoxydiol to Submicron Aerosol Particles. *Environ. Sci. Technol.* **2014**, *48* (19), 11178–11186.
- (8) Weber, R. J.; Guo, H.; Russell, A. G.; Nenes, A. High aerosol acidity despite declining atmospheric sulfate concentrations over the past 15 years. *Nat. Geosci.* **2016**, 9 (4), 282–285.
- (9) Guo, H.; Liu, J.; Froyd, K. D.; Roberts, J. M.; Veres, P. R.; Hayes, P. L.; Jimenez, J. L.; Nenes, A.; Weber, R. J. Fine particle pH and gas—particle phase partitioning of inorganic species in Pasadena, California, during the 2010 CalNex campaign. *Atmos. Chem. Phys.* 2017, 17 (9), 5703–5719.
- (10) Frauenheim, M.; Offenberg, J.; Zhang, Z.; Surratt, J. D.; Gold, A. The C5-Alkene Triol Conundrum: Structural Characterization and Quantitation of Isoprene-Derived C5H10O3 Reactive Uptake Products. *Environ. Sci. Technol. Lett.* **2022**, *9* (10), 829-836.
- (11) Jang, M. C.; Czoschke, N. M.; Lee, S.; Kamens, R. M. Heterogeneous Atmospheric Aerosol Production by Acid-Catalyzed Particle-Phase Reactions. *Science* **2002**, 298, 814–817.
- (12) Lin, Y.-H.; Zhang, Z.; Docherty, K. S.; Zhang, H.; Budisulistiorini, S. H.; Rubitschun, C. L.; Shaw, S. L.; Knipping, E. M.; Edgerton, E. S.; Kleindienst, T. E.; Gold, A.; Surratt, J. D. Isoprene Epoxydiols as Precursors to Secondary Organic Aerosol Formation: Acid-Catalyzed Reactive Uptake Studies with Authentic Compounds. *Environ. Sci. Technol.* 2012, 46 (1), 250–258.
- (13) Ault, A. P. Aerosol Acidity: Novel Measurements and Implications for Atmospheric Chemistry. *Acc. Chem. Res.* **2020**, *53* (9), 1703–1714.
- (14) Guo, H.; Xu, L.; Bougiatioti, A.; Cerully, K. M.; Capps, S. L.; Hite, J. R.; Carlton, A. G.; Lee, S. H.; Bergin, M. H.; Ng, N. L.; Nenes, A.; Weber, R. J. Fine-particle water and pH in the southeastern United States. *Atmos. Chem. Phys.* **2015**, *15* (9), 5211–5228.
- (15) Yao, X.; Ling, T. Y.; Fang, M.; Chan, C. K. Size dependence of in situ pH in submicron atmospheric particles in Hong Kong. *Atmos. Environ.* **2007**, *41* (2), 382–393.
- (16) Behera, S. N.; Betha, R.; Liu, P.; Balasubramanian, R. A study of diurnal variations of PM2.5 acidity and related chemical species using a new thermodynamic equilibrium model. *Sci. Total Environ.* **2013**, 452–453, 286–295.
- (17) Hallquist, M.; Wenger, J. C.; Baltensperger, U.; Rudich, Y.; Simpson, D.; Claeys, M.; Dommen, J.; Donahue, N. M.; George, C.; Goldstein, A. H.; Hamilton, J. F.; Herrmann, H.; Hoffmann, T.; Iinuma, Y.; Jang, M.; Jenkin, M. E.; Jimenez, J. L.; Kiendler-Scharr, A.; Maenhaut, W.; McFiggans, G.; Mentel, T. F.; Monod, A.; Prévôt, A. S. H.; Seinfeld, J. H.; Surratt, J. D.; Szmigielski, R.; Wildt, J. The formation, properties and impact of secondary organic aerosol: current and emerging issues. *Atmos. Chem. Phys.* **2009**, 9 (14), 5155–5236.
- (18) Guenther, A. B.; Jiang, X.; Heald, C. L.; Sakulyanontvittaya, T.; Duhl, T.; Emmons, L. K.; Wang, X. The Model of Emissions of Gases and Aerosols from Nature version 2.1 (MEGAN2.1): an extended and updated framework for modeling biogenic emissions. *Geosci. Model Dev.* 2012, 5 (6), 1471–1492.
- (19) Wennberg, P. O.; Bates, K. H.; Crounse, J. D.; Dodson, L. G.; McVay, R. C.; Mertens, L. A.; Nguyen, T. B.; Praske, E.; Schwantes, R. H.; Smarte, M. D.; St Clair, J. M.; Teng, A. P.; Zhang, X.; Seinfeld, J. H. Gas-Phase Reactions of Isoprene and Its Major Oxidation Products. *Chem. Rev.* **2018**, *118* (7), 3337–3390.
- (20) Claeys, M.; Graham, B.; Vas, G.; Wang, W.; Vermeylen, R.; Pashynska, V.; Cafmeyer, J.; Guyon, P.; Andreae, M. O.; Artaxo, P.; Maenhaut, W. Formation of Secondary Organic Aerosols Through Photooxidation of Isoprene. *Science* **2004**, *303*, 1173–1176.

- (21) Kroll, J. H.; Ng, N. L.; Murphy, S. M.; Flagan, R. C.; Seinfeld, J. H. Secondary Organic Aerosol Formation from Isoprene Photo-oxidation. *Environ. Sci. Technol.* **2006**, *40* (6), 1869–1877.
- (22) Surratt, J. D.; Murphy, S. M.; Kroll, J. H.; Ng, N. L.; Hildebrandt, L.; Sorooshian, A.; Szmigielski, R.; Vermeylen, R.; Maenhaut, W.; Claeys, M.; Flagan, R. C.; Seinfeld, J. H. Chemical Composition of Secondary Organic Aerosol Formed from the Photooxidation of Isoprene. *J. Phys. Chem. A* **2006**, *110* (31), 9665–9690.
- (23) Paulot, F.; Crounse, J. D.; Kjaergaard, H. G.; Kürten, A.; St. Clair, J. M.; Seinfeld, J. H.; Wennberg, P. O. Unexpected Epoxide Formation in the Gas-Phase Photooxidation of Isoprene. *Science* **2009**, 325 (5941), 730–733.
- (24) Bates, K. H.; Crounse, J. D.; St. Clair, J. M.; Bennett, N. B.; Nguyen, T. B.; Seinfeld, J. H.; Stoltz, B. M.; Wennberg, P. O. Gas Phase Production and Loss of Isoprene Epoxydiols. *J. Phys. Chem. A* **2014**, *118* (7), 1237–1246.
- (25) Surratt, J. D.; Gómez-González, Y.; Chan, A. W. H.; Vermeylen, R.; Shahgholi, M.; Kleindienst, T. E.; Edney, E. O.; Offenberg, J. H.; Lewandowski, M.; Jaoui, M.; Maenhaut, W.; Claeys, M.; Flagan, R. C.; Seinfeld, J. H. Organosulfate Formation in Biogenic Secondary Organic Aerosol. *J. Phys. Chem. A* **2008**, *112* (36), 8345–8378.
- (26) Surratt, J. D.; Chan, A. W. H.; Eddingsaas, N. C.; Chan, M.; Loza, C. L.; Kwan, A. J.; Hersey, S. P.; Flagan, R. C.; Wennberg, P. O.; Seinfeld, J. H. Reactive intermediates revealed in secondary organic aerosol formation from isoprene. *Proc. Natl. Acad. Sci. U. S. A.* **2010**, 107 (15), 6640–6645.
- (27) Cui, T.; Zeng, Z.; Dos Santos, E. O.; Zhang, Z.; Chen, Y.; Zhang, Y.; Rose, C. A.; Budisulistiorini, S. H.; Collins, L. B.; Bodnar, W. M.; De Souza, R. A. F.; Martin, S. T.; Machado, C. M. D.; Turpin, B. J.; Gold, A.; Ault, A. P.; Surratt, J. D. Development of a hydrophilic interaction liquid chromatography (HILIC) method for the chemical characterization of water-soluble isoprene epoxydiol (IEPOX)-derived secondary organic aerosol. *Environ. Sci.: Processes Impacts* **2018**, *20* (11), 1524–1536.
- (28) Glasius, M.; Bering, M. S.; Yee, L. D.; De Sá, S. S.; Isaacman-Vanwertz, G.; Wernis, R. A.; Barbosa, H. M. J.; Alexander, M. L.; Palm, B. B.; Hu, W.; Campuzano-Jost, P.; Day, D. A.; Jimenez, J. L.; Shrivastava, M.; Martin, S. T.; Goldstein, A. H. Organosulfates in aerosols downwind of an urban region in central Amazon. *Environ. Sci.: Processes Impacts* **2018**, *20* (11), 1546–1558.
- (29) Hettiyadura, A. P. S.; Al-Naiema, I. M.; Hughes, D. D.; Fang, T.; Stone, E. A. Organosulfates in Atlanta, Georgia: anthropogenic influences on biogenic secondary organic aerosol formation. *Atmos. Chem. Phys.* **2019**, *19* (5), 3191–3206.
- (30) Hettiyadura, A. P. S.; Jayarathne, T.; Baumann, K.; Goldstein, A. H.; De Gouw, J. A.; Koss, A.; Keutsch, F. N.; Skog, K.; Stone, E. A. Qualitative and quantitative analysis of atmospheric organosulfates in Centreville, Alabama. *Atmos. Chem. Phys.* **2017**, *17* (2), 1343–1359.
- (31) Xu, L.; Guo, H.; Boyd, C. M.; Klein, M.; Bougiatioti, A.; Cerully, K. M.; Hite, J. R.; Isaacman-Vanwertz, G.; Kreisberg, N. M.; Knote, C.; Olson, K.; Koss, A.; Goldstein, A. H.; Hering, S. V.; De Gouw, J.; Baumann, K.; Lee, S. -H.; Nenes, A.; Weber, R. J.; Ng, N. L. Effects of anthropogenic emissions on aerosol formation from isoprene and monoterpenes in the southeastern United States. *Proc. Natl. Acad. Sci. U. S. A.* 2015, 112 (1), 37–42.
- (32) Aoki, E.; Sarrimanolis, J. N.; Lyon, S. A.; Elrod, M. J. Determining the Relative Reactivity of Sulfate, Bisulfate, and Organosulfates with Epoxides on Secondary Organic Aerosol. ACS Earth Space Chem. 2020, 4 (10), 1793–1801.
- (33) Mekic, M.; Brigante, M.; Vione, D.; Gligorovski, S. Exploring the ionic strength effects on the photochemical degradation of pyruvic acid in atmospheric deliquescent aerosol particles. *Atmos. Environ.* **2018**, *185*, 237–242.
- (34) Mekic, M.; Gligorovski, S. Ionic strength effects on heterogeneous and multiphase chemistry: Clouds versus aerosol particles. *Atmos. Environ.* **2021**, 244, 117911.
- (35) Fountoukis, C.; Nenes, A. ISORROPIA II: a computationally efficient thermodynamic equilibrium model for K+-Ca2+-Mg2+-

- NH+-Na+-SO2--NO--Cl--H2O aerosols. *Atmos. Chem. Phys.* **2007**, *7* (17), 4639-4659.
- (36) Herrmann, H.; Schaefer, T.; Tilgner, A.; Styler, S. A.; Weller, C.; Teich, M.; Otto, T. Tropospheric aqueous-phase chemistry: kinetics, mechanisms, and its coupling to a changing gas phase. *Chem. Rev.* 2015, 115 (10), 4259–4334.
- (37) Dickson, A. G.; Wesolowski, D. J.; Palmer, D. A.; Mesmer, R. E. Dissociation constant of bisulfate ion in aqueous sodium chloride solutions to 250.degree.C. J. Phys. Chem. 1990, 94 (20), 7978–7985.
- (38) Pitzer, K. S. Ř.; Roy, R. N.; Silvester, L. F. Thermodynamics of Electrolytes. 7. Sulfuric Acid. *J. Am. Chem. Soc.* **1977**, 99 (15), 4930–4936.
- (39) Hefter, G.; Gumiński, C. Remarks on the Evaluation of Thermodynamic Data for Sulfate Ion Protonation. *J. Solution Chem.* **2019**, 48 (11–12), 1657–1670.
- (40) Zhang, J.; Liu, J.; Ding, X.; He, X.; Zhang, T.; Zheng, M.; Choi, M.; Isaacman-Vanwertz, G.; Yee, L.; Zhang, H.; Misztal, P.; et al. New formation and fate of Isoprene SOA markers revealed by field data-constrained modeling. *Npj Clim. Atmos. Sci.* **2023**, *6* (1), 69.
- (41) Shrivastava, M.; Rasool, Q. Z.; Zhao, B.; Octaviani, M.; Zaveri, R. A.; Zelenyuk, A.; Gaudet, B.; Liu, Y.; Shilling, J. E.; Schneider, J.; Schulz, C.; Zöger, M.; Martin, S. T.; Ye, J.; Guenther, A.; Souza, R. F.; Wendisch, M.; Pöschl, U Tight Coupling of Surface and In-Plant Biochemistry and Convection Governs Key Fine Particulate Components over the Amazon Rainforest. ACS Earth Space Chem. 2022, 6 (2), 380–390.
- (42) Eddingsaas, N. C.; Vandervelde, D. G.; Wennberg, P. O. Kinetics and Products of the Acid-Catalyzed Ring-Opening of Atmospherically Relevant Butyl Epoxy Alcohols. *J. Phys. Chem. A* **2010**, *114* (31), 8106–8113.
- (43) Zhang, Z.; Lin, Y. H.; Zhang, H.; Surratt, J. D.; Ball, L. M.; Gold, A. Technical Note: Synthesis of isoprene atmospheric oxidation products: isomeric epoxydiols and the rearrangement products cisand trans -3-methyl-3,4-dihydroxytetrahydrofuran. *Atmos. Chem. Phys.* **2012**, *12* (18), 8529–8535.
- (44) Zhang, Y.; Chen, Y.; Lei, Z.; Olson, N. E.; Riva, M.; Koss, A. R.; Zhang, Z.; Gold, A.; Jayne, J. T.; Worsnop, D. R.; Onasch, T. B.; Kroll, J. H.; Turpin, B. J.; Ault, A. P.; Surratt, J. D. Joint Impacts of Acidity and Viscosity on the Formation of Secondary Organic Aerosol from Isoprene Epoxydiols (IEPOX) in Phase Separated Particles. *ACS Earth Space Chem.* **2019**, 3 (12), 2646–2658.
- (45) Cooke, M. E.; Armstrong, N. C.; Lei, Z.; Chen, Y.; Waters, C. M.; Zhang, Y.; Buchenau, N. A.; Dibley, M. Q.; Ledsky, I. R.; Szalkowski, T.; Lee, J. Y.; Baumann, K.; Zhang, Z.; Vizuete, W.; Gold, A.; Surratt, J. D.; Ault, A. P. Organosulfate Formation in Proxies for Aged Sea Spray Aerosol: Reactive Uptake of Isoprene Epoxydiols to Acidic Sodium Sulfate. ACS Earth Space Chem. 2022, 6 (12), 2790–2800.
- (46) Riva, M.; Chen, Y.; Zhang, Y.; Lei, Z.; Olson, N. E.; Boyer, H. C.; Narayan, S.; Yee, L. D.; Green, H. S.; Cui, T.; Zhang, Z.; Baumann, K.; Fort, M.; Edgerton, E.; Budisulistiorini, S. H.; Rose, C. A.; Ribeiro, I. O.; E Oliveira, R. L.; Dos Santos, E. O.; Machado, C. M. D.; Szopa, S.; Zhao, Y.; Alves, E. G.; De Sá, S. S.; Hu, W.; Knipping, E. M.; Shaw, S. L.; Duvoisin Junior, S.; De Souza, R. A. F.; Palm, B. B.; Jimenez, J.-L.; Glasius, M.; Goldstein, A. H.; Pye, H. O. T.; Gold, A.; Turpin, B. J.; Vizuete, W.; Martin, S. T.; Thornton, J. A.; Dutcher, C. S.; Ault, A. P.; Surratt, J. D. Increasing Isoprene Epoxydiol-to-Inorganic Sulfate Aerosol Ratio Results in Extensive Conversion of Inorganic Sulfate to Organosulfur Forms: Implications for Aerosol Physicochemical Properties. *Environ. Sci. Technol.* 2019, 53 (15), 8682—8694.
- (47) Craig, R. L.; Peterson, P. K.; Nandy, L.; Lei, Z.; Hossain, M. A.; Camarena, S.; Dodson, R. A.; Cook, R. D.; Dutcher, C. S.; Ault, A. P. Direct Determination of Aerosol pH: Size-Resolved Measurements of Submicrometer and Supermicrometer Aqueous Particles. *Anal. Chem.* **2018**, *90* (19), 11232–11239.
- (48) Lin, Y.-H.; Budisulistiorini, S. H.; Chu, K.; Siejack, R. A.; Zhang, H.; Riva, M.; Zhang, Z.; Gold, A.; Kautzman, K. E.; Surratt, J. D. Light-Absorbing Oligomer Formation in Secondary Organic

- Aerosol from Reactive Uptake of Isoprene Epoxydiols. Environ. Sci. Technol. 2014, 48 (20), 12012–12021.
- (49) Darer, A. I.; Cole-Filipiak, N. C.; O'Connor, A. E.; Elrod, M. J. Formation and stability of atmospherically relevant isoprene-derived organosulfates and organonitrates. *Environ. Sci. Technol.* **2011**, 45 (5), 1895–1902.
- (50) Chen, Y.; Zhang, Y.; Lambe, A. T.; Xu, R.; Lei, Z.; Olson, N. E.; Zhang, Z.; Szalkowski, T.; Cui, T.; Vizuete, W.; Gold, A.; Turpin, B. J.; Ault, A. P.; Chan, M. N.; Surratt, J. D. Heterogeneous Hydroxyl Radical Oxidation of Isoprene-Epoxydiol-Derived Methyltetrol Sulfates: Plausible Formation Mechanisms of Previously Unexplained Organosulfates in Ambient Fine Aerosols. *Environ. Sci. Technol. Lett.* **2020**, *7* (7), 460–468.
- (51) Clegg, S. L.; Brimblecombe, P.; Wexler, A. S. Thermodynamic Model of the System H+–NH4+–SO42-–NO3-–H2O at Tropospheric Temperatures. *J. Phys. Chem. A* **1998**, *102* (12), 2137–2154.
- (52) Wexler, A. S.; Clegg, S. L. Atmospheric aerosol models for systems including the ions H+, NH 4+, Na+, SO 4 2-, NO 3-, Cl-, Br-, and H 2 O. *J. Geophys. Res.* **2002**, *107* (D14), ACH14-1–ACH 14-14.
- (53) Clegg, S. L.; Seinfeld, J. H.; Brimblecombe, P. Thermodynamic modelling of aqueous aerosols containing electrolytes and dissolved organic compounds. *J. Aerosol Sci.* **2001**, *32*, 713–738.
- (54) Surratt, J. D.; Kroll, J. H.; Kleindienst, T. E.; Edney, E. O.; Claeys, M.; Sorooshian, A.; Ng, N. L.; Offenberg, J. H.; Lewandowski, M.; Jaoui, M.; Flagan, R. C.; Seinfeld, J. H. Evidence for Organosulfates in Secondary Organic Aerosol. *Environ. Sci. Technol.* **2007**, *41* (2), 517–527.
- (55) D'Ambro, E. L.; Schobesberger, S.; Gaston, C. J.; Lopez-Hilfiker, F. D.; Lee, B. H.; Liu, J.; Zelenyuk, A.; Bell, D.; Cappa, C. D.; Helgestad, T.; Li, Z.; Guenther, A.; Wang, J.; Wise, M.; Caylor, R.; Surratt, J. D.; Riedel, T.; Hyttinen, N.; Salo, V.-T.; Hasan, G.; Kurtén, T.; Shilling, J. E.; Thornton, J. A. Chamber-based insights into the factors controlling epoxydiol (IEPOX) secondary organic aerosol (SOA) yield, composition, and volatility. *Atmos. Chem. Phys.* **2019**, *19* (17), 11253–11265.
- (56) Lopez-Hilfiker, F. D.; Mohr, C.; D'Ambro, E. L.; Lutz, A.; Riedel, T. P.; Gaston, C. J.; Iyer, S.; Zhang, Z.; Gold, A.; Surratt, J. D.; Lee, B. H.; Kurten, T.; Hu, W. W.; Jimenez, J.; Hallquist, M.; Thornton, J. A. Molecular Composition and Volatility of Organic Aerosol in the Southeastern U.S.: Implications for IEPOX Derived SOA. *Environ. Sci. Technol.* **2016**, *50* (5), 2200–2209.
- (57) Wallace, B. J.; Mongeau, M. L.; Zuend, A.; Preston, T. C. Impact of pH on Gas-Particle Partitioning of Semi-Volatile Organics in Multicomponent Aerosol. *Environ. Sci. Technol.* **2023**, *57* (44), 16974–16988.
- (58) Riedel, T. P.; Lin, Y.-H.; Budisulistiorini, S. H.; Gaston, C. J.; Thornton, J. A.; Zhang, Z.; Vizuete, W.; Gold, A.; Surratt, J. D. Heterogeneous Reactions of Isoprene-Derived Epoxides: Reaction Probabilities and Molar Secondary Organic Aerosol Yield Estimates. *Environ. Sci. Technol. Lett.* **2015**, *2* (2), 38–42.
- (59) McNeill, V. F.; Woo, J. L.; Kim, D. D.; Schwier, A. N.; Wannell, N. J.; Sumner, A. J.; Barakat, J. M. Aqueous-Phase Secondary Organic Aerosol and Organosulfate Formation in Atmospheric Aerosols: A Modeling Study. *Environ. Sci. Technol.* **2012**, *46* (15), 8075–8081.
- (60) Marais, E. A.; Jacob, D. J.; Jimenez, J. L.; Campuzano-Jost, P.; Day, D. A.; Hu, W.; Krechmer, J.; Zhu, L.; Kim, P. S.; Miller, C. C.; Fisher, J. A.; Travis, K.; Yu, K.; Hanisco, T. F.; Wolfe, G. M.; Arkinson, H. L.; Pye, H. O. T.; Froyd, K. D.; Liao, J.; McNeill, V. F. Aqueous-phase mechanism for secondary organic aerosol formation from isoprene: application to the Southeast United States and cobenefit of SO(2) emission controls. *Atmos. Chem. Phys.* **2016**, *16* (3), 1603–1618.
- (61) Budisulistiorini, S. H.; Nenes, A.; Carlton, A. G.; Surratt, J. D.; McNeill, V. F.; Pye, H. O. T. Simulating Aqueous-Phase Isoprene-Epoxydiol (IEPOX) Secondary Organic Aerosol Production During the 2013 Southern Oxidant and Aerosol Study (SOAS). *Environ. Sci. Technol.* 2017, 51 (9), 5026–5034.